
DyJR: Preserving Diversity in Reinforcement Learning with Verifiable Rewards via Dynamic Jensen-Shannon Replay

Long Li^{1*} Zhijian Zhou^{2,3*} Tianyi Wang⁴ Weidi Xu⁵ Zuming Huang⁵ Wei Chu⁵ Zhe Wang¹
 Shirui Pan^{1†} Chao Qu^{2,6†} Yuan Qi^{2,6}

Abstract

While Reinforcement Learning (RL) enhances Large Language Model reasoning, on-policy algorithms like GRPO are sample-inefficient as they discard past rollouts. Existing experience replay methods address this by reusing accurate samples for direct policy updates, but this often incurs high computational costs and causes mode collapse via overfitting. We argue that historical data should prioritize sustaining *diversity* rather than simply reinforcing *accuracy*. To this end, we propose *Dynamic Jensen-Shannon Replay (DyJR)*, a simple yet effective regularization framework using a dynamic reference distribution from recent trajectories. DyJR introduces two innovations: (1) A Time-Sensitive Dynamic Buffer that uses FIFO and adaptive sizing to retain only temporally proximal samples, synchronizing with model evolution; and (2) Jensen-Shannon Divergence Regularization, which replaces direct gradient updates with a distributional constraint to prevent diversity collapse. Experiments on mathematical reasoning and Text-to-SQL benchmarks demonstrate that DyJR significantly outperforms GRPO as well as baselines such as RLEP and Ex-GRPO, while maintaining training efficiency comparable to the original GRPO. Furthermore, from the perspective of Rank- k token probability evolution, we show that DyJR enhances diversity and mitigates over-reliance on Rank-1 tokens, elucidating how specific sub-modules of DyJR influence the training dynamics.

* Equal contribution. † Co-corresponding authors. ¹Griffith University, Australia ²Fudan University, China ³Shanghai Innovation Institute, China ⁴Beijing University of Post and Telecommunications ⁵INFLY TECH, China ⁶Shanghai Academy of Artificial Intelligence for Science, China. Correspondence to: Long Li <long.li@griffithuni.edu.au>.

1. Introduction

Reasoning capability is central to Artificial General Intelligence in the large language models (LLMs) era (OpenAI, 2023; Yang et al., 2025; Zhu et al., 2025a). Models like OpenAI o1 demonstrate that Reinforcement Learning (RL) transcends preference alignment by enhancing logic through long Chain-of-Thought (CoT) exploration (OpenAI, 2024; Guo et al., 2025). While “long thinking” via Verifiable Rewards is now mainstream (Chen et al., 2025b), a key bottleneck exists: the on-policy nature of current Reinforcement Learning with Verifiable Reward (RLVR) (Cai et al., 2025; Cai & Sugiyama, 2026) algorithms causes expensive rollout data to be discarded after a single update (Shao et al., 2024; Zhan et al., 2025). This inefficiency wastes vast resources and prevents learning from past successes, hindering the scalability of RL in reasoning tasks (Fu et al., 2025; Zhou et al., 2026).

Experience Replay (Rolnick et al., 2019; Mnih et al., 2013; Lillicrap, 2015; Liu et al., 2026) has recently been adapted for LLM training to improve sample efficiency. Methods such as ReMix (Liang et al., 2025), RePO (Li et al., 2025b), Ex-GRPO (Zhan et al., 2025), and RLEP (Zhang et al., 2025) reuse historical trajectories by following a data augmentation paradigm. These approaches typically maintain massive buffers to store historical samples and treat them as additional positive instances for direct policy gradient updates. Formally, they optimize a joint objective $\mathcal{J}(\theta) = \mathcal{J}_{\text{on}}(\theta) + \alpha \mathcal{J}_{\text{exp}}(\theta)$ using the same standard clipped surrogate objective for both terms.¹

We contend that this mainstream approach suffers from *two core misconceptions*. First, indiscriminate forward updates exacerbate mode collapse. By directly maximizing the likelihood of historical trajectories, the model is coerced into over-fitting specific solution paths (Zhu et al., 2025b; Peng et al., 2025), leading to a swift erosion of its exploratory potential (Wang et al., 2025; Yue et al., 2025; Cheng et al.,

¹Specifically, $\mathcal{J}_{\text{exp}}(\theta)$ takes the exact same form as the on-policy objective: $\mathbb{E}_{q \sim \mathcal{B}_{\text{exp}}}[\min(r(\theta)\hat{A}, \text{clip}(r(\theta), 1 - \epsilon, 1 + \epsilon)\hat{A})]$, where $r(\theta) = \frac{\pi_{\theta}}{\pi_{\text{old}}}$. This effectively treats replayed trajectories as additional off-policy samples.

2025). Second, traditional Experience Replay methods necessitate substantial training resources for sample storage and reuse; for instance, approaches like RLEP incur massive GPU memory overhead by archiving the entire trajectory history. In contrast, our empirical findings suggest that historical data is not uniformly valuable, as RL training exhibits a *rapid transition window* where the model’s entropy decreases sharply during the early stages (typically the first 20 steps) before converging to a peaked distribution. Consequently, by prioritizing large-scale sample storage exclusively during this volatile initial phase while maintaining a minimal footprint in later stages, one can achieve performance comparable to continuous large-scale storage while drastically reducing memory requirements.

Based on these observations, we redefine the role of Experience Replay in reasoning tasks: the objective should shift from accuracy optimization via correct samples to a regularization mechanism for sustaining diversity. Guided by this philosophy, we propose the Dynamic Jensen-Shannon Replay Algorithm (*DyJR*). Unlike previous approaches, *DyJR* introduces two key innovations. Regarding **data construction**, we replace brute-force storage with a non-uniform dynamic buffer strategy. Specifically, we implement a dynamic capacity mechanism that expands the buffer to retain a larger volume of samples during the rapid transition phase—thereby capturing high-entropy reasoning patterns—and subsequently contracts it. Crucially, we employ a First-In-First-Out (FIFO) protocol for buffer updates, retaining only samples that are most temporally proximal to the current model. Empirical evidence indicates that while retaining excessive historical data with large temporal variance impedes learning, utilizing temporally adjacent data minimizes training resource consumption while yielding optimal performance. Regarding **data utilization**, we move away from direct policy gradient updates and introduce Jensen-Shannon divergence as a regularization constraint. By treating the mixture of historical policies as a dynamic distributional anchor, we minimize the Jensen-Shannon divergence between the current policy and this mixture. This prevents the model from drifting away from diverse successful paths without aggressively altering the optimization direction.

Our main contributions are summarized as follows:

(1) **Redefining the Replay Paradigm: From Accuracy Optimization to Diversity Regularization.** We demonstrate that the primary value of replayed data lies in sustaining diversity rather than merely reinforcing accuracy. Consequently, we replace direct gradient updates with a Jensen-Shannon divergence distributional constraint, effectively preserving the model’s exploration capability and robustness.

(2) **Proposing a Dynamic Data Construction Strategy Based on Temporal Proximity.** We introduce a non-

uniform dynamic buffer mechanism that expands storage during the rapid transition phase to capture high-entropy patterns and contracts it as the model stabilizes. By employing a FIFO protocol to retain only the most temporally adjacent samples, we achieve optimal performance while minimizing training resource consumption.

(3) **Extensive Experiments and Fine-Grained Analysis.** We demonstrate robust improvements across diverse tasks (e.g., Math and Text-to-SQL) and architectures (Qwen and Llama families), achieving substantial gains in both Pass@1 and Pass@k with negligible GPU memory overhead. Furthermore, we provide a detailed ablation analysis from the perspective of Rank-*k* token probability evolution to elucidate how *DyJR*’s sub-modules influence training dynamics.

2. Preliminaries

In this section, we formalize the RLVR setup and introduce the foundational algorithms: Group Relative Policy Optimization (GRPO) and JS divergence.

2.1. RL Backbone: GRPO

We formulate the reasoning task as a Markov Decision Process (MDP). Given a query x , a policy π_θ generates a reasoning chain $y = (y_1, \dots, y_L)$. The environment returns a binary reward $r(x, y) \in \{0, 1\}$.

Standard PPO requires a value function critic, which is computationally expensive for LLMs. Instead, we utilize GRPO (Shao et al., 2024), which estimates baselines using group statistics. For each query x , GRPO samples a group of G outputs $\{y_1, \dots, y_G\}$ from the old policy $\pi_{\theta_{old}}$. The advantage for the i -th output is computed as:

$$\hat{A}_i = \frac{r(x, y_i) - \mu_{group}}{\sigma_{group}} \tag{1}$$

where μ_{group} and σ_{group} are the mean and standard deviation of rewards within the group. The GRPO objective maximizes the surrogate loss:

$$\mathcal{L}_{GRPO}(\theta) = -\frac{1}{G} \sum_{i=1}^G \min \left(\rho_i \hat{A}_i, \text{clip}(\rho_i, 1 - \epsilon, 1 + \epsilon) \hat{A}_i \right) \tag{2}$$

where $\rho_i = \frac{\pi_\theta(y_i|x)}{\pi_{\theta_{old}}(y_i|x)}$ is the importance sampling ratio.

2.2. Forward KL Divergence

In contrast to symmetric measures, the Forward Kullback-Leibler (KL) divergence is a standard asymmetric metric typically minimized in maximum likelihood estimation. For a target distribution P and an approximating distribution Q , it is defined as:

$$D_{KL}(P||Q) = \mathbb{E}_{x \sim P} \left[\ln \frac{P(x)}{Q(x)} \right] \tag{3}$$

The Forward KL is characterized by its **mode-covering** behavior. Because the expectation is taken with respect to the reference distribution P , the divergence penalizes Q severely if $Q(x)$ is small where $P(x)$ is large. Consequently, minimizing $D_{\text{KL}}(P\|Q)$ forces Q to spread its probability mass to cover all modes of P , ensuring broad support even if it results in assigning mass to low-probability regions of the target distribution.

2.3. Jensen-Shannon Divergence

The Jensen-Shannon divergence offers a symmetrized and smoothed alternative to the KL divergence. For two probability distributions P and Q , the JS divergence is defined via a mixture distribution $M = \frac{1}{2}(P + Q)$ as:

$$D_{\text{JS}}(P\|Q) = \frac{1}{2}D_{\text{KL}}(P\|M) + \frac{1}{2}D_{\text{KL}}(Q\|M) \quad (4)$$

Unlike the standard KL divergence, which is asymmetric and unbounded (potentially approaching infinity if the support of Q does not fully encompass P), the JS divergence is symmetric and bounded within $[0, \ln 2]$.

3. Method

We now introduce DyJR. While GRPO provides efficient exploration, it is prone to mode collapse in sparse-reward settings. DyJR mitigates this by maintaining a **Dynamic Replay Buffer** and applying a **JS Regularization** term derived from the definition in Sec. 2.

Algorithm 1 DyJR

- 1: **Input:** Dataset \mathcal{D} , Policy π_θ , Max Age M , Reg Coefficient α_{JS} .
 - 2: **Initialize:** Buffer $\mathcal{S} \leftarrow \emptyset$.
 - 3: **for** step $t = 1, \dots, T$ **do**
 - 4: **Rollout:** Sample queries X , generate group $Y \sim \pi_{\theta_{\text{old}}}(X)$.
 - 5: **Eval:** Compute rewards R and group confidence C_{id} .
 - 6: **Buffer Maintenance:**
 - 7: 1. Evict samples where age $> M$.
 - 8: 2. Select new samples based on C_{id} and schedule η (Eq. 6).
 - 9: 3. Store $(x, y, \log \pi_{\theta_{\text{old}}})$ into \mathcal{S} .
 - 10: **Optimization:**
 - 11: Calculate $\mathcal{L}_{\text{GRPO}}$ on online batch (X, Y) using Eq. (2).
 - 12: Sample batch B_{replay} uniformly from \mathcal{S} .
 - 13: Calculate \mathcal{L}_{JS} on B_{replay} using Eq. (7)-(9).
 - 14: Update θ minimizing $\mathcal{L}_{\text{GRPO}} + \alpha_{\text{JS}}\mathcal{L}_{\text{JS}}$.
 - 15: **end for**
-

3.1. Dynamic Reference Construction

To leverage historical success, we construct a reference distribution $Q_{\mathcal{B}}$ supported by a Replay Buffer \mathcal{S}_t .

Dynamic Replay Buffer To address the *non-stationarity* of the policy, we enforce a **Max Age** (M) constraint. The buffer strictly retains only perfect samples ($r = 1$) generated within the last M steps. To enable efficient divergence computation without re-forwarding, we store the token-level log-probabilities computed at generation time. A buffer entry is defined as $(x_k, y_k, \log \pi_{\text{old}}^{(k)})$. At step t , any stale sample is evicted:

$$\mathcal{S}_t = \{(x_k, y_k, \log \pi_{\text{old}}^{(k)}) \mid r(y_k) = 1, t - T_{id_k} \leq M\} \quad (5)$$

This ensures the reference distribution tightly tracks the shifting capability boundary of the current policy π_θ .

Bias-Aware Adaptive Data Selection To mitigate the selection bias inherent in filtering exclusively for correctness while ensuring robust coverage across varying task difficulties, we propose a **confidence-stratified descending admission strategy**. For each query in batch B_t , we define the *empirical confidence* C_{id} as the count of correct responses among G sampled paths. We strictly prioritize high-confidence samples by iteratively admitting perfect trajectories where $C_{id} = k$, sweeping k from G down to 1:

$$\mathcal{P}_t^{\text{new}} \leftarrow \mathcal{P}_t^{\text{new}} \cup \{(x, y, \log \pi_{\text{old}}) \in B_t \mid C_{id} = k, r(y) = 1\} \quad (6)$$

This process halts once the newly admitted samples reach the target fill rate η (default 5%). This ‘‘High-to-Low’’ mechanism inherently provides a **difficulty-adaptive** property: (1) For Easy Tasks, it preferentially secures high-confidence samples ($C_{id} \approx G$), ensuring a low-variance reference; (2) For Hard Tasks, it naturally relaxes admission criteria to capture rare solutions ($C_{id} \ll G$), thereby preventing data starvation and the ‘‘catastrophic forgetting’’ of difficult capabilities.

Mitigating Early Diversity Collapse A critical challenge in RLVR is the rapid collapse of policy entropy during early training stages, often occurring before the replay buffer is sufficiently populated. To counteract this, we implement a Time-Aware Adaptive Schedule. During the initial warm-up phase (e.g., the first 20 steps), we temporarily elevate the target fill rate η from 5% to 20%. By proactively admitting a broader spectrum of exploratory samples during initialization, this strategy rapidly diversifies the reference distribution, effectively smoothing the optimization trajectory and safeguarding against premature mode collapse.

3.2. JS Regularization Implementation

We apply JS divergence to regularize π_θ towards the buffer distribution Q_B . While Eq. (3) gives the theoretical definition, computing standard JS divergence implies calculating the mixture distribution M , which is intractable for autoregressive models.

Instead, we employ a low-variance generative estimator (Wang et al., 2023). For a sample s drawn from \mathcal{S}_t , we compute the probability ratio u_s using the current policy and the stored log-probabilities:

$$u_s^{(j)} = \exp\left(\log \pi_\theta(y_s^{(j)}|x_s, y_s^{(<j)}) - \log \pi_{\text{old}}^{(j)}\right) \quad (7)$$

The contribution term $f(u_s)$ approximating the JS divergence is:

$$f(u_s) = u_s \log u_s - (u_s + 1) \log \frac{u_s + 1}{2} \quad (8)$$

The practical regularization loss is then averaged over a sampled replay batch B_{replay} :

$$\mathcal{L}_{\text{JS}}(\theta) = \frac{1}{|B_{\text{replay}}|} \sum_{s \in B_{\text{replay}}} \frac{1}{L_s} \sum_{j=1}^{L_s} f(u_s^{(j)}) \quad (9)$$

3.3. Joint Optimization Objective

The proposed DyJR algorithm integrates the on-policy GRPO objective with the JS regularization. The total loss is:

$$\mathcal{L}_{\text{total}}(\theta) = \mathcal{L}_{\text{GRPO}}(\theta) + \alpha_{\text{JS}} \cdot \mathcal{L}_{\text{JS}}(\theta) \quad (10)$$

where α_{JS} is hyperparameter of regularization coefficient. This objective encourages the model to explore higher-reward solutions via GRPO while the JS regularization term acts as a flexible anchor to preserve the diversity of historical successful modes. The full procedure is summarized in Algorithm 1.

4. Experiments

4.1. Setting

In this section, we conduct extensive experiments to evaluate the capabilities of DyJR across diverse scenarios. We design two distinct types of tasks: (1) **Long-chain Mathematical Reasoning (6k Response Length)**: utilizing the Qwen3-4B-Base model, we train on the Reinforce-Ada-Hard (Xiong et al., 2025) subset—a collection of 14k high-difficulty samples—and evaluate on 6 competition-level benchmarks to observe performance breakthroughs at extreme reasoning depths; and (2) **SQL Generation**: employing Llama-3.1-8B-Instruct on the BIRD (Li et al., 2024b) dataset, with evaluations conducted across both BIRD and Spider (Yu et al.,

2018) to assess cross-domain generalization and moderate-difficulty logic.

These two tasks comprehensively validate the effectiveness and robustness of our method from three dimensions: the extremity of reasoning depth, the heterogeneity of cross-domain tasks, and the variance in initial model capabilities. Detailed experimental configurations and hyperparameter settings are provided in Appendix B.

4.2. Baseline

The baseline methods for comparison primarily include: **GRPO** without the KL term, **DAPO** (Yu et al., 2025), and **DPH-RL** (Li et al., 2025a) which similarly utilizes JS divergence. Additionally, we compare against **ExGRPO** (Zhan et al., 2025) and **RLEP** (Zhang et al., 2025), both of which incorporate a replay buffer mechanism. To ensure a fair and consistent comparison, we set the ϵ_{high} parameter to 0.28 across all experiments.

4.3. Main Results

We present a comprehensive evaluation of our proposed method, DyJR, across six mathematical reasoning benchmarks with varying difficulty levels. Table 1 reports the performance comparison between DyJR and the primary baseline, GRPO, as well as other representative methods. As shown in Table 1, DyJR (configured with $\alpha_{\text{JS}} = 0.05$, $M = 8$) achieves a remarkable average accuracy of 34.1%. This represents a substantial improvement of 4.3% over the GRPO baseline (29.8%). Crucially, this performance gain is robust across the difficulty spectrum. Whether on the relatively simpler AMC23 benchmark (where we observe a +7.4% boost over GRPO) or on the extremely challenging HMMT25 dataset (with a +2.9% improvement), DyJR consistently demonstrates significant superiority. This indicates that our method effectively enhances reasoning capabilities regardless of the problem complexity.

Compare with Other Methods. We explicitly compare our dynamic approach with DPH-RL, which employs a static Jensen-Shannon constraint mechanism. While DPH-RL improves upon the baseline, it lags behind DyJR (31.3% vs. 34.1%). We attribute this to the inherent nature of mathematical datasets, which exhibit high variance in reasoning paths and complexity. A static constraint coefficient fails to adapt to these fluctuations, often acting as an inflexible bottleneck that limits the model’s potential. In contrast, our dynamic adjustment mechanism allows the model to flexibly balance alignment and exploration, leading to superior convergence. Furthermore, we conducted a comparative analysis with other replay buffer-based methods. RLEP yielded the poorest performance, primarily because it necessitates storing two correct solutions for each query. In our experiments, this required archiving approximately 28k

Table 1. Performance comparison on various mathematical benchmarks. Best results are bolded. We report the mean and standard deviation across three independent runs for GRPO and DyJR (denoted in blue parentheses). Note that **Minerva*** is reported as Mean@16, while all other benchmarks are evaluated using Mean@256.

Model	AIME25	AMC23	Beyond AIME	BRUMO25	HMMT25	Minerva*	Avg
Qwen3-4B-Base (Mean@256)							
<i>Baselines</i>							
Base Model	8.2	51.5	4.3	16.6	1.9	29.0	18.6
GRPO	19.1 (± 1.8)	64.6 (± 1.5)	10.7 (± 0.9)	29.6 (± 1.6)	9.8 (± 0.8)	45.2 (± 1.4)	29.8
DAPO	21.5	65.5	10.6	30.4	9.2	47.8	30.8
<i>Other Methods</i>							
RLEP	23.0	68.9	10.6	28.9	10.8	48.4	31.7
Ex-GRPO	21.7	70.2	11.6	32.8	10.4	50.1	32.8
DPH-RL	22.8	65.2	10.8	30.1	10.5	48.1	31.3
<i>Our Results (DyJR)</i>							
DyJR ($\alpha_{JS} = 0.05, M = 8$)	23.1 (± 1.6)	72.0 (± 1.1)	12.7 (± 0.7)	33.4 (± 1.4)	12.7 (± 0.8)	50.4 (± 2.6)	34.1
<i>Ablation-Divergence</i>							
Forward KL	22.8	70.7	11.3	32.6	10.5	47.3	32.5
<i>Ablation-α</i>							
$\alpha_{JS} = 0.01$	22.5	69.3	11.5	31.0	12.5	49.5	32.7
$\alpha_{JS} = 0.2$	21.4	66.7	10.1	29.0	10.9	47.4	30.9
<i>Ablation-M</i>							
$M = 16$	23.6	69.3	11.3	31.0	13.6	48.8	32.9
$M = 32$	22.0	68.9	10.9	30.2	10.3	47.7	31.7
$M = 64$	21.3	67.9	10.5	29.3	9.7	46.9	30.9

QA pairs. In contrast, DyJR theoretically requires storing only 2k pairs, demonstrating a significant advantage in efficiency. Meanwhile, Ex-GRPO outperformed RLEP; we attribute this to its tendency to select samples based on entropy, which indirectly preserves diversity. This observation aligns closely with the perspective proposed in our work.

Justification for JS Divergence To justify our selection of the JS divergence as the regularization metric, we compared the standard Forward KL divergence against our JS-based approach. As shown in Table 1, the JS-based DyJR significantly outperforms the Forward KL variant (34.1% vs. 32.5%). We attribute this performance gap to the heterogeneous nature of the replay buffer, which consists of a mixture of samples from rapidly evolving policies rather than a single stationary distribution. In this complex setting, the Forward KL divergence ($D_{KL}(P_{data}||\pi_{\theta})$) is known to be *mode-covering*, which tends to force the policy to average across all diverse samples in the buffer. This often leads to over-smoothing and training instability under significant distributional shifts. Conversely, the symmetric and bounded nature of the JS divergence ensures a more robust and balanced regularization signal. By measuring the distance between distributions and their mixture mean, JS divergence effectively mitigates aggressive mode-matching behaviors and provides stable alignment even with multi-source, non-stationary data. We further analyze this phenomenon by

visualizing the specific training dynamics in Section 5.1.

It is worth noting that we exclude the Reverse KL divergence from our comparison for two primary reasons. First, prior studies have indicated that Reverse KL is less effective at preserving distributional diversity than Forward KL (Li et al., 2025a; Deng et al., 2025), occasionally even underperforming baselines that omit KL regularization entirely (Yu et al., 2025). Second, the computation of Reverse KL requires sampling from the current policy π_{θ} , whereas the samples in the replay buffer are generated by historical policies. This mismatch violates the fundamental requirements for employing Reverse KL in this context, rendering it unsuitable for our framework.

Sensitivity to Regularization Coefficient The coefficient α_{JS} governs the strength of the regularization constraint, and we observe that performance follows an inverted U-shaped trajectory with respect to this parameter. The model achieves optimal performance (34.1%) at $\alpha_{JS} = 0.05$. Reducing α_{JS} to 0.01 leads to a performance drop to 32.7%, likely due to under-regularization, where the model drifts too far from the reference policy without sufficient guidance. Conversely, increasing α_{JS} to 0.2 results in a marked degradation to 30.9%, suggesting that excessive regularization overly constrains the policy, hindering its ability to explore and discover optimal reasoning paths.

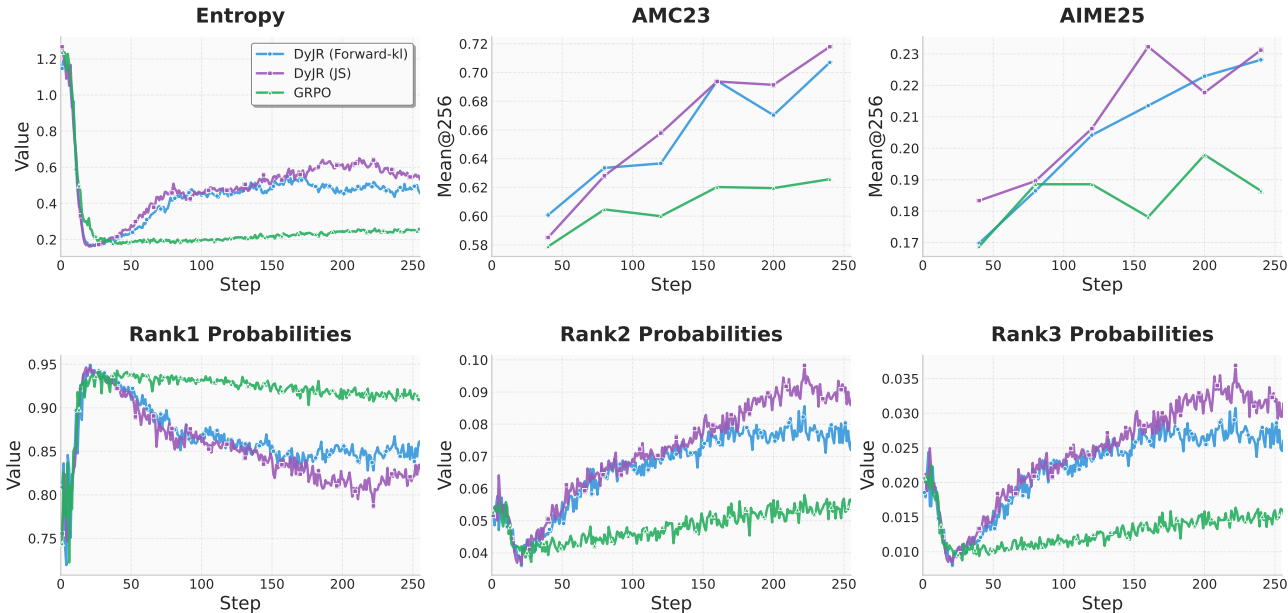


Figure 1. We track the evolution of the Qwen3-4B-Base model throughout the training process. The recorded metrics include the entropy of the output distribution, the average probability of rank- k tokens ($P_{\text{rank-}k}$), and the performance fluctuations on the evaluation datasets.

Impact of Max Age (M) We further investigated the scalability of DyJR with respect to the Max Age M . Interestingly, our empirical results favor a smaller Max Age for this objective, with performance peaking at $M = 8$ (34.1%). As M increases to 16, 32, and 64, we observe a monotonic decline in average accuracy to 32.9%, 31.7%, and 30.9%, respectively. This finding suggests that for the DyJR framework, a constrained Max Age is advantageous, possibly by ensuring data freshness and mitigating the policy divergence (or distribution shift) that arises when updating on samples generated by significantly older model states.

4.4. Experiments on SQL Tasks

To evaluate the generalization capabilities of our proposed framework beyond mathematical reasoning, we conducted additional experiments on Text-to-SQL tasks using the Llama-3-8B model as the backbone. We selected two widely used benchmarks, BIRD and Spider, reporting both Pass@1 accuracy and Pass@16.

Table 2. Comparison of different models.

Model	Bird		Spider	
	Pass@1	Pass@16	Pass@1	Pass@16
GRPO	59.4	68.4	72.5	80.3
DAPO	60.1	69.2	71.5	79.4
DPH-RL	62.8	72.4	76.0	84.1
DyJR	62.7	72.9	77.5	87.3

As shown in Table 2, the static Jensen-Shannon divergence-

based method, DPH-RL, demonstrates strong performance in the SQL domain, achieving notable improvements in both Pass@1 and pass@ k metrics. However, as noted in previous sections, its effectiveness is limited in the rapidly evolving mathematical domain, where its gains in mean@256 are marginal. In contrast, DyJR exhibits superior adaptability across diverse tasks. It not only maintains robustness in mathematical reasoning but also achieves state-of-the-art results in SQL tasks. Specifically, DyJR outperforms the strong baseline GRPO by a significant margin, improving Pass@1 accuracy by +3.3% on BIRD and +5.0% on Spider, while boosting Pass@16 by +4.5% and +7.0%, respectively. These results underscore the universality and effectiveness of our dynamic joint reasoning strategy.

5. Analysis

5.1. Evolution of Diversity During Training

To investigate the dynamics of generation diversity throughout the training process, we visualized the evolution of entropy and the selection probabilities of rank- k tokens for GRPO, DyJR (Forward KL), a variant where JS is replaced by Forward KL, and the proposed DyJR (JS).

Metric Definitions: Following the evaluation protocols established in prior work (Peng et al., 2025), we quantify the uncertainty and diversity of the model’s output distribution using *Approximate Entropy* and *Average Probability* based on the top- k log-probabilities. For each generated token x_t ,

the approximate entropy is calculated as:

$$H(x_t) \approx - \sum_{i=1}^k \tilde{p}_i \log \tilde{p}_i, \quad \text{where} \quad \tilde{p}_i = \frac{\exp(\ell_i)}{\sum_{j=1}^k \exp(\ell_j)} \quad (11)$$

Here, \tilde{p}_i represents the normalized probability derived from the log-probability ℓ_i of the i -th ranked token. Additionally, to gauge the model’s confidence in specific ranks, we compute the average probability of rank- k tokens across all generated tokens, defined as $\bar{P}_{\text{rank-}k} = \frac{1}{N} \sum_{n=1}^N \exp(\ell_{\text{rank-}k}^{(n)})$.

Analysis of Training Dynamics. As shown in Figure 1, the probability distribution of rank- k tokens serves as a direct indicator of whether the model suffers from mode collapse. As illustrated in Figure 1, GRPO exhibits a sharp decline in entropy during the initial phase, characterized by a rapid surge in Rank-1 probability to near 1.0. Crucially, this probability consistently remains above 90% throughout the entire training trajectory. This pattern indicates a severe imbalance where the model becomes overly confident in a single reasoning path, effectively losing its exploration capability. This observation aligns with our main results, where GRPO converges early but stagnates at a lower performance plateau due to entrapment in local optima.

In contrast, DyJR demonstrates a more healthy dynamic. While it also experiences an initial entropy drop to adapt to reward signals, it avoids collapsing into a low-entropy state. Instead, DyJR gradually retreats from the extreme Rank-1 dominance, redistributing probability mass to Rank-2 and Rank-3 tokens. This *rebalancing* process signifies that the model retains the capacity to explore alternative reasoning paths while maintaining high confidence. Notably, the entropy of DyJR continues to rise even after 200 steps, suggesting sustained diversity growth and further potential for performance improvement. Due to the influence of data from diverse sources, the mode-covering Forward KL, while preserving more diversity than GRPO, consistently exhibits a performance gap compared to DyJR which utilizes JS divergence. This further corroborates the conclusions drawn from our ablation studies.

5.2. From RLEP to DyJR

To provide a granular analysis of the individual components within DyJR, we illustrate the systematic transition from the baseline RLEP to the DyJR framework, specifically focusing on the evolution of $\bar{P}_{\text{rank-}k}$. We conduct a comparative evaluation across three experimental configurations: (1) **Original RLEP:** The standard baseline implementation of Replay-enhanced Policy Optimization. (2) **RLEP with Dynamic Reference Construction:** The sampling mechanism is fully replaced with our *Dynamic Reference Construction* strategy, while the data utilization protocol in the replay buffer remains identical to that of RLEP. (3) **DyJR:** Our

complete proposed method, integrating both *Dynamic Reference Construction* and the full *Regularized Rehearsal* mechanism. The results are illustrated in Figure 2.

Compared to the Original RLEP, which maintains the highest rank-1 probability, we observe a gradual decline in its confidence during the later stages of training. Unlike GRPO, Original RLEP can still access diverse historical samples due to the extensive time span of its replay buffer. The RLEP with Dynamic Reference Construction significantly outperforms the original baseline by exhibiting higher distributional diversity. This demonstrates that our dynamic reference strategy is superior to the naive preservation of all historical data. We hypothesize that the utility of replay buffer data is highly sensitive to its “distance” from the current policy; samples from the distant past, even when used for policy updates, are often effectively discarded by the PPO-clipping mechanism as they deviate too far from the current distribution π_θ . Finally, DyJR consistently maintains the highest level of diversity throughout the training process. This confirms that our *Regularized Rehearsal* (via JS divergence) is substantially more effective than simply using buffer data for standard policy updates. Collectively, these results validate the efficacy of DyJR from the perspectives of both data construction and utilization.

5.3. Large-Scale Pass@k Evaluation

We evaluated the performance of various methods as the sampling budget k scales up to 1024. As illustrated in Figure 3a, the standard GRPO baseline consistently underperforms; it lags behind DyJR even at lower k values and exhibits sluggish growth in Pass@ k as the budget increases. In contrast, DyJR (utilizing JS divergence) demonstrates superior scalability, effectively leveraging larger sampling budgets to achieve continuous performance gains. Regarding the divergence analysis, while the DyJR (Forward KL) variant yields higher performance than the GRPO baseline, it remains consistently inferior to the JS-based DyJR across the entire range of k . Overall, DyJR emerges as the optimal method, showcasing robust capability in maximizing performance through large-scale sampling.

5.4. Complexity Analysis

The proposed algorithm is designed with a focus on high scalability and efficiency. For **space complexity**, by strictly bounding the buffer capacity to $N \times \eta \times M$, the storage footprint remains minimal. In our experimental setup ($N = 4096, \eta = 5\%, M = 8$), the maximum buffer size contains approximately 1,638 sequences. Given an average context length of 6k tokens, the total storage requirement is roughly 9.8×10^6 tokens. The GPU memory overhead incurred by storing these sequence indices is negligible (significantly less than 1GB under float16 precision) compared

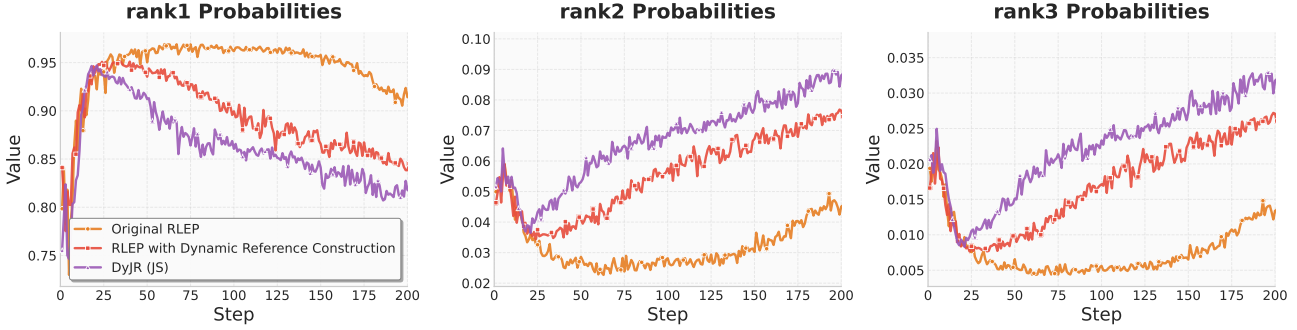


Figure 2. Comparison of rank- k trends across the transition from RLEP to DyJR.

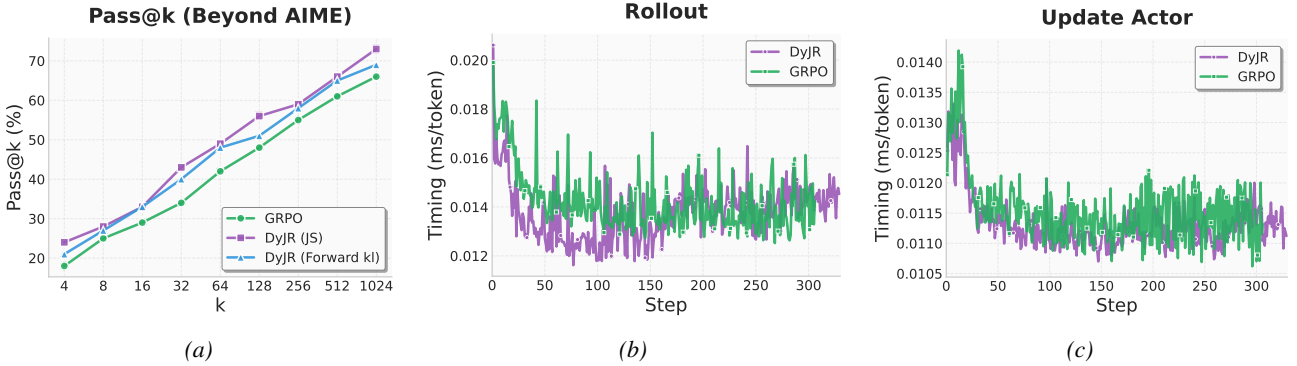


Figure 3. (a) Pass@ k performance on the **Beyond AIME** dataset across varying sampling budgets k . (b) and (c) Computational latency comparison between DyJR (w/o KL) and GRPO during the *Rollout* phase and the *Actor Update* phase (encompassing log-probability calculation, forward passes, and gradient updates), respectively.

to the memory consumed by model weights and optimizer states. Furthermore, since the replay batch size is merely a fraction of the online batch size, the impact on peak activation memory during training is minimal. For **time complexity**, the additional computational cost arises primarily from the forward and backward passes required to compute the regularization term $\mathcal{L}_{\text{SFT}}(\theta)$ on the replayed samples. Given that the number of replayed samples (configured as 512 in our experiments) is significantly smaller than the online training batch size (4,096), this theoretically results in only a marginal increase in wall-clock time per training step. As demonstrated in our computational efficiency experiments (see Figure 3b and 3c), the overall training throughput maintains a level of efficiency consistent with the original GRPO across both the rollout and update phases.

6. Related Work

Experience Replay in LLM Training Originally from off-policy reinforcement learning (Mnih et al., 2013; Lillicrap, 2015), experience replay has been adapted for LLMs to enhance efficiency, as seen in off-policy methods like ReMix (Liang et al., 2025) and RePO (Li et al., 2025b). Others, such as RLEP (Zhang et al., 2025) and ExGRPO (Zhan et al., 2025), focus on reusing high-quality historical trajec-

tories. While ARPO (Lu et al., 2025) integrates replay with GRPO, most existing methods neglect proper importance weighting or divergence constraints, resulting in distribution mismatch—a critical gap our work addresses.

Diversity Maintenance in LLM RL To counteract the rapid collapse of policy diversity in RLVR (Agarwal et al., 2025; Cheng et al., 2025; Tan et al., 2025), researchers have employed entropy regularization techniques (Wang et al., 2025; Chen et al., 2025a). Recent works like SimKO (Peng et al., 2025) and W-REINFORCE (Zhu et al., 2025b) mitigate this by differentiating the processing of positive and negative samples to prevent distribution narrowing. Furthermore, DPH-RL (Li et al., 2025a) adopts the f -divergence family as a robust alternative to standard reverse-KL.

7. Conclusion

In this paper, we introduced DyJR, which fundamentally redefines the role of Experience Replay in reasoning tasks, proposing a paradigm shift from merely reinforcing accuracy to actively sustaining diversity. By implementing a time-sensitive dynamic buffer that prioritizes retaining early high-entropy samples, and utilizing JS divergence as a distributional constraint, DyJR effectively prevents the model

from converging to narrow solution paths without introducing the prohibitive computational costs of traditional replay methods. Our analysis of training dynamics reveals a critical insight: the primary value of historical data lies in the rich exploration patterns inherent in the early training stages, rather than the high-accuracy trajectories of the later stages. By preserving this early diversity, DyJR maintains a healthy Rank-token distribution and mitigates over-reliance on a single reasoning path.

Impact Statement

This paper presents work whose goal is to advance the field of Machine Learning. There are many potential societal consequences of our work, none which we feel must be specifically highlighted here.

References

- Agarwal, S., Zhang, Z., Yuan, L., Han, J., and Peng, H. The unreasonable effectiveness of entropy minimization in llm reasoning, 2025. URL <https://arxiv.org/abs/2505.15134>.
- Balunović, M., Dekoninck, J., Petrov, I., Jovanović, N., and Vechev, M. Matharena: Evaluating llms on uncontaminated math competitions, February 2025. URL <https://matharena.ai/>.
- Cai, X.-Q. and Sugiyama, M. Vi-curl: Stabilizing verifier-independent rl reasoning via confidence-guided variance reduction. *arXiv preprint arXiv:2602.12579*, 2026.
- Cai, X.-Q., Wang, W., Liu, F., Liu, T., Niu, G., and Sugiyama, M. Reinforcement learning with verifiable yet noisy rewards under imperfect verifiers. *arXiv preprint arXiv:2510.00915*, 2025.
- Chen, M., Chen, G., Wang, W., and Yang, Y. Seed-grpo: Semantic entropy enhanced grpo for uncertainty-aware policy optimization, 2025a. URL <https://arxiv.org/abs/2505.12346>.
- Chen, Q., Qin, L., Liu, J., Peng, D., Guan, J., Wang, P., Hu, M., Zhou, Y., Gao, T., and Che, W. Towards reasoning era: A survey of long chain-of-thought for reasoning large language models. *arXiv preprint arXiv:2503.09567*, 2025b.
- Cheng, D., Huang, S., Zhu, X., Dai, B., Zhao, W. X., Zhang, Z., and Wei, F. Reasoning with exploration: An entropy perspective on reinforcement learning for llms, 2025. URL <https://arxiv.org/abs/2506.14758>.
- Deng, W., Wei, L., Yu, C., and Wu, T. Unlocking reasoning capabilities in llms via reinforcement learning exploration. *arXiv preprint arXiv:2510.03865*, 2025.
- Fu, W., Gao, J., Shen, X., Zhu, C., Mei, Z., He, C., Xu, S., Wei, G., Mei, J., Wang, J., Yang, T., Yuan, B., and Wu, Y. Areal: A large-scale asynchronous reinforcement learning system for language reasoning, 2025. URL <https://arxiv.org/abs/2505.24298>.
- Guo, D., Yang, D., Zhang, H., Song, J., Zhang, R., Xu, R., Zhu, Q., Ma, S., Wang, P., Bi, X., et al. Deepseek-r1: Incentivizing reasoning capability in llms via reinforcement learning. *arXiv preprint arXiv:2501.12948*, 2025.
- Lambert, N., Morrison, J., Pyatkin, V., Huang, S., Ivison, H., Brahman, F., Miranda, L. J. V., Liu, A., Dziri, N., Lyu, S., Gu, Y., Malik, S., Graf, V., Hwang, J. D., Yang, J., Bras, R. L., Taffjord, O., Wilhelm, C., Soldaini, L., Smith, N. A., Wang, Y., Dasigi, P., and Hajishirzi, H. Tulu 3: Pushing frontiers in open language model post-training, 2025. URL <https://arxiv.org/abs/2411.15124>.
- Lewkowycz, A., Andreassen, A., Dohan, D., Dyer, E., Michalewski, H., Ramasesh, V. V., Slone, A., Anil, C., Schlag, I., Gutman-Solo, T., Wu, Y., Neyshabur, B., Gur-Ari, G., and Misra, V. Solving quantitative reasoning problems with language models. In *NeurIPS*, 2022.
- Li, J., Beeching, E., Tunstall, L., Lipkin, B., Soletskyi, R., Huang, S., Rasul, K., Yu, L., Jiang, A. Q., Shen, Z., et al. Numinamath: The largest public dataset in ai4maths with 860k pairs of competition math problems and solutions. *Hugging Face repository*, 13(9):9, 2024a.
- Li, J., Hui, B., Qu, G., Yang, J., Li, B., Li, B., Wang, B., Qin, B., Geng, R., Huo, N., et al. Can llm already serve as a database interface? a big bench for large-scale database grounded text-to-sqls. *Advances in Neural Information Processing Systems*, 36, 2024b.
- Li, L., He, X., Wang, H., Wang, L., and He, L. How do humans write code? large models do it the same way too. In Al-Onaizan, Y., Bansal, M., and Chen, Y.-N. (eds.), *Proceedings of the 2024 Conference on Empirical Methods in Natural Language Processing*, pp. 4638–4649, Miami, Florida, USA, November 2024c. Association for Computational Linguistics. doi: 10.18653/v1/2024.emnlp-main.267. URL <https://aclanthology.org/2024.emnlp-main.267/>.
- Li, L., Hao, J., Liu, J. K., Zhou, Z., Miao, Y., Pang, W., Tan, X., Chu, W., Wang, Z., Pan, S., et al. The choice of divergence: A neglected key to mitigating diversity collapse in reinforcement learning with verifiable reward. *arXiv preprint arXiv:2509.07430*, 2025a.
- Li, S., Zhou, Z., Lam, W., Yang, C., and Lu, C. Repo: Replay-enhanced policy optimization. *arXiv preprint arXiv:2506.09340*, 2025b.

- Liang, J., Tang, H., Ma, Y., Liu, J., Zheng, Y., Hu, S., Bai, L., and Hao, J. Squeeze the soaked sponge: Efficient off-policy reinforcement finetuning for large language model. *arXiv preprint arXiv:2507.06892*, 2025.
- Lillicrap, T. P. Continuous control with deep reinforcement learning. *arXiv preprint arXiv:1509.02971*, 2015.
- Liu, W., Wu, H., Kuang, Y., Han, X., Zhong, T., Feng, J., and Lu, W. Automated optimization modeling via a localizable error-driven perspective. *arXiv preprint arXiv:2602.11164*, 2026.
- Lu, F., Zhong, Z., Liu, S., Fu, C.-W., and Jia, J. Arpo: End-to-end policy optimization for gui agents with experience replay. *arXiv preprint arXiv:2505.16282*, 2025.
- Meta AI. Introducing meta Llama 3: The most capable openly available LLM to date, April 2024. URL <https://ai.meta.com/blog/meta-llama-3/>. Accessed: 2024-04-18.
- Mnih, V., Kavukcuoglu, K., Silver, D., Graves, A., Antonoglou, I., Wierstra, D., and Riedmiller, M. Playing atari with deep reinforcement learning. *arXiv preprint arXiv:1312.5602*, 2013.
- OpenAI. GPT4 technical report. *arXiv preprint arXiv:2303.08774*, 2023.
- OpenAI. Learning to reason with llms, 2024. URL <https://openai.com/index/learning-to-reason-with-llms/>.
- Peng, R., Ren, Y., Yu, Z., Liu, W., and Wen, Y. Simko: Simple pass@k policy optimization. *arXiv preprint arXiv:2510.14807*, 2025.
- Rolnick, D., Ahuja, A., Schwarz, J., Lillicrap, T., and Wayne, G. Experience replay for continual learning. *Advances in neural information processing systems*, 32, 2019.
- Shao, Z., Wang, P., Zhu, Q., Xu, R., Song, J., Zhang, M., Li, Y., Wu, Y., and Guo, D. Deepseekmath: Pushing the limits of mathematical reasoning in open language models. *arXiv preprint arXiv:2402.03300*, 2024.
- Tan, Y., Wang, M., He, S., Liao, H., Zhao, C., Lu, Q., Liang, T., Zhao, J., and Liu, K. Bottom-up policy optimization: Your language model policy secretly contains internal policies. *arXiv preprint arXiv:2512.19673*, 2025. URL <https://arxiv.org/abs/2512.19673>.
- Team, K., Du, A., Gao, B., Xing, B., Jiang, C., Chen, C., Li, C., Xiao, C., Du, C., Liao, C., Tang, C., Wang, C., Zhang, D., Yuan, E., Lu, E., Tang, F., Sung, F., Wei, G., Lai, G., Guo, H., Zhu, H., Ding, H., Hu, H., Yang, H., Zhang, H., Yao, H., Zhao, H., Lu, H., Li, H., Yu, H., Gao, H., Zheng, H., Yuan, H., Chen, J., Guo, J., Su, J., Wang, J., Zhao, J., Zhang, J., Liu, J., Yan, J., Wu, J., Shi, L., Ye, L., Yu, L., Dong, M., Zhang, N., Ma, N., Pan, Q., Gong, Q., Liu, S., Ma, S., Wei, S., Cao, S., Huang, S., Jiang, T., Gao, W., Xiong, W., He, W., Huang, W., Xu, W., Wu, W., He, W., Wei, X., Jia, X., Wu, X., Xu, X., Zu, X., Zhou, X., Pan, X., Charles, Y., Li, Y., Hu, Y., Liu, Y., Chen, Y., Wang, Y., Liu, Y., Qin, Y., Liu, Y., Yang, Y., Bao, Y., Du, Y., Wu, Y., Wang, Y., Zhou, Z., Wang, Z., Li, Z., Zhu, Z., Zhang, Z., Wang, Z., Yang, Z., Huang, Z., Huang, Z., Xu, Z., Yang, Z., and Lin, Z. Kimi k1.5: Scaling reinforcement learning with llms, 2025. URL <https://arxiv.org/abs/2501.12599>.
- Team, Q. Qwen2.5: A party of foundation models, September 2024. URL <https://qwenlm.github.io/blog/qwen2.5/>.
- Team, Q. Qwq-32b: Embracing the power of reinforcement learning, 2025.
- Wang, C., Jiang, Y., Yang, C., Liu, H., and Chen, Y. Beyond reverse kl: Generalizing direct preference optimization with diverse divergence constraints. *ArXiv*, abs/2309.16240, 2023. URL <https://api.semanticscholar.org/CorpusID:263142109>.
- Wang, S., Yu, L., Gao, C., Zheng, C., Liu, S., Lu, R., Dang, K., Chen, X., Yang, J., Zhang, Z., Liu, Y., Yang, A., Zhao, A., Yue, Y., Song, S., Yu, B., Huang, G., and Lin, J. Beyond the 80/20 rule: High-entropy minority tokens drive effective reinforcement learning for llm reasoning, 2025. URL <https://arxiv.org/abs/2506.01939>.
- Xiong, W., Ye, C., Liao, B., Dong, H., Xu, X., Monz, C., Bian, J., Jiang, N., and Zhang, T. Reinforce-ada: An adaptive sampling framework under non-linear rl objectives, 2025. URL <https://arxiv.org/abs/2510.04996>.
- Yang, A., Li, A., Yang, B., Zhang, B., Hui, B., Zheng, B., Yu, B., Gao, C., Huang, C., Lv, C., Zheng, C., Liu, D., Zhou, F., Huang, F., Hu, F., Ge, H., Wei, H., Lin, H., Tang, J., Yang, J., Tu, J., Zhang, J., Yang, J., Yang, J., Zhou, J., Zhou, J., Lin, J., Dang, K., Bao, K., Yang, K., Yu, L., Deng, L., Li, M., Xue, M., Li, M., Zhang, P., Wang, P., Zhu, Q., Men, R., Gao, R., Liu, S., Luo, S., Li, T., Tang, T., Yin, W., Ren, X., Wang, X., Zhang, X., Ren, X., Fan, Y., Su, Y., Zhang, Y., Zhang, Y., Wan, Y., Liu, Y., Wang, Z., Cui, Z., Zhang, Z., Zhou, Z., and Qiu, Z. Qwen3 technical report, 2025. URL <https://arxiv.org/abs/2505.09388>.
- Yu, Q., Zhang, Z., Zhu, R., Yuan, Y., Zuo, X., Yue, Y., Dai, W., Fan, T., Liu, G., Liu, L., Liu, X., Lin, H., Lin,

- Z., Ma, B., Sheng, G., Tong, Y., Zhang, C., Zhang, M., Zhang, W., Zhu, H., Zhu, J., Chen, J., Chen, J., Wang, C., Yu, H., Song, Y., Wei, X., Zhou, H., Liu, J., Ma, W.-Y., Zhang, Y.-Q., Yan, L., Qiao, M., Wu, Y., and Wang, M. Dapo: An open-source llm reinforcement learning system at scale, 2025. URL <https://arxiv.org/abs/2503.14476>.
- Yu, T., Zhang, R., Yang, K., Yasunaga, M., Wang, D., Li, Z., Ma, J., Li, I., Yao, Q., Roman, S., et al. Spider: A large-scale human-labeled dataset for complex and cross-domain semantic parsing and text-to-sql task. In *Proceedings of the 2018 Conference on Empirical Methods in Natural Language Processing*, pp. 3911–3921, 2018.
- Yue, Y., Chen, Z., Lu, R., Zhao, A., Wang, Z., Yue, Y., Song, S., and Huang, G. Does reinforcement learning really incentivize reasoning capacity in LLMs beyond the base model? In *2nd AI for Math Workshop @ ICML 2025*, 2025. URL <https://openreview.net/forum?id=upehLVgqlb>.
- Zhan, R., Li, Y., Wang, Z., Qu, X., Liu, D., Shao, J., Wong, D. F., and Cheng, Y. Exgrpo: Learning to reason from experience. *arXiv preprint arXiv:2510.02245*, 2025.
- Zhang, H., Fu, J., Zhang, J., Fu, K., Wang, Q., Zhang, F., and Zhou, G. Rlep: Reinforcement learning with experience replay for llm reasoning. *arXiv preprint arXiv:2507.07451*, 2025.
- Zhou, Y., Li, Y., Cheng, D., Fan, H., and Cheng, Y. Look inward to explore outward: Learning temperature policy from llm internal states via hierarchical rl. *arXiv preprint arXiv:2602.13035*, 2026.
- Zhu, C., Lin, Y., Chen, S., Wang, Y., and Lin, J. Medeyes: Learning dynamic visual focus for medical progressive diagnosis. *arXiv preprint arXiv:2511.22018*, 2025a.
- Zhu, X., Xia, M., Wei, Z., Chen, W.-L., Chen, D., and Meng, Y. The surprising effectiveness of negative reinforcement in llm reasoning. *arXiv preprint arXiv:2506.01347*, 2025b.

A. Additional Related Work

Reinforcement Learning with Verifiable Rewards RLVR (Yue et al., 2025; Lambert et al., 2025) has emerged as a cornerstone for enhancing the reasoning capabilities of LLMs in domains with objective ground truth, such as mathematics and coding (Shao et al., 2024; Guo et al., 2025; Team, 2024; Li et al., 2024c). Following the paradigm established by models like OpenAI o1 (OpenAI, 2024) and DeepSeek-R1 (Guo et al., 2025), recent efforts such as QwQ (Team, 2025) and Kimi k1.5 (Team et al., 2025) have leveraged verifiable feedback to scale test-time compute. While effective, standard RLVR typically relies on on-policy optimization, which often suffers from sample inefficiency and training instability when dealing with long-sequence reasoning trajectories.

B. Experiment Setups

Table 3. Experimental settings adopted in this work. We employ the AdamW optimizer with $\beta_1 = 0.9$, $\beta_2 = 0.95$ and a weight decay of 0.1. The gradient clipping threshold is set to 1.0 for all models.

Category	Parameters	GRPO	DAPO	DPH-RL	DyJR	RLEP
Inference	G (Group Size)	8	8	8	8	8
	Prompt Batch Size	512	512	512	512	512
	Temperature	1.0	1.0	1.0	1.0	1.0
	Top- p / Top- k	1.0 / -1	1.0 / -1	1.0 / -1	1.0 / -1	1.0 / -1
	Validation Temp	0.7	0.7	0.7	0.7	0.7
	Validation Top- p	0.95	0.95	0.95	0.95	0.95
	Response Length	6144	6144	6144	6144	6144
Training	Clip Ratio High (ϵ)	0.28	0.28	0.28	0.28	0.28
	Clip Ratio Low (ϵ)	0.2	0.2	0.2	0.2	0.2
	Learning Rate	2×10^{-5}				
	Mini Batch Size	128	128	128	128	128
	Loss Agg. Mode	token-mean	token-mean	token-mean	token-mean	token-mean
	Dynamic Sampling	False	True	True	False	False
	Replay Bsz	-	-	512	512	512
	Correct Threshold	-	-	6 of 8	-	-
	Max Age (M)	-	-	-	8	-
	Regularization Coefficient	-	-	0.2	0.05	-
Hardware	GPU Count	$32 \times$ A800				
	Parallel (TP/SP)	1 / 1	1 / 1	1 / 1	1 / 1	1 / 1

We design two distinct types of tasks: (1) A **long-chain mathematical reasoning task** based on the Qwen3-4B-Base (Yang et al., 2025) model. For training, we utilize Reinforce-Ada-Hard (Xiong et al., 2025), a high-difficulty subset of 14k samples filtered from the OpenR1-Math-220k² dataset, specifically excluding simpler prompts with an average success rate (average reward > 0.375). Evaluation is performed on highly challenging benchmarks, including AIME25 (Li et al., 2024a), HMMT25 (Balunović et al., 2025), BRUMO25 (Balunović et al., 2025), AMC23, Minerva (Lewkowycz et al., 2022) and Beyond AIME. This task is designed to observe the significant performance leap from a low baseline to high-level proficiency following RL training. (2) A **SQL generation task** based on Llama-3.1-8B-Instruct (Meta AI, 2024), which focuses on moderate-difficulty reasoning typically within a 1k token limit. The model is trained on the BIRD (Li et al., 2024b) dataset and evaluated across both BIRD and Spider (Yu et al., 2018) datasets to test cross-domain performance.

In this work, we employ multiple experimental setups to validate the effectiveness of **DyJR** in comparison with baseline methods; Table 3 summarizes the detailed configurations for all setups. Specifically, *Replay Bsz* denotes the batch size of newly added data items during each data fusion step. For **DPH-RL**, following the experimental protocol in their original work, we incorporate samples that yield 6 correct responses out of 8 sampled paths into the regularization term. Regarding **RLEP**, we preserve two correct solution trajectories for each query q in the replay buffer. These buffered samples are subsequently treated as data generated by the current policy π_θ and integrated into the joint policy update process.

²<https://huggingface.co/datasets/open-r1/OpenR1-Math-220k>

Table 4. ExGRPO-specific hyperparameters for experience replay.

Parameter	Value	Description
Replay ratio (ρ)	0.5	Fraction of replay samples in each mini-batch
Delayed replay threshold	0.35	Minimum batch Pass@1 required to activate experience replay
Difficulty bucket range	[0, 7]	Bounds for difficulty-based bucketing (k/K)
Replay metric	Entropy	Criterion for evaluating trajectory quality
Trajectory selection mode	Argmin	Select the lowest-entropy successful trajectory per prompt

For Pass@1, we employ greedy decoding (i.e., temperature $T = 0$). For Mean@256, we generate 256 samples with a temperature of $T = 0.7$ and calculate the average accuracy across all samples.

ExGRPO. (Experiential Group Relative Policy Optimization) (Zhan et al., 2025) extends GRPO with an experience replay framework that integrates *experience management* and *mixed optimization*. During training, ExGRPO maintains an experience pool that maps each prompt to a set of previously successful solution trajectories, and categorizes prompts into difficulty buckets according to their most recent rollout accuracy. To prevent overfitting to trivial cases, prompts whose rollouts are entirely correct are moved into a *retired set* and excluded from subsequent replay.

At each update step, ExGRPO applies a replay ratio ρ to partition each mini-batch into on-policy samples and replayed experiences. Difficulty buckets are sampled using a Gaussian weighting centered at 0.5, thereby emphasizing prompts of intermediate difficulty. For each selected prompt, ExGRPO further selects the successful trajectory with the lowest entropy under the current policy, encouraging stable exploitation while mitigating excessive diversity collapse.

The additional hyperparameters introduced by ExGRPO are summarized in Table 4, while all other training configurations follow the GRPO baseline in the Table 3.

C. The Irreplaceability of Early Exploration

Table 5. Performance of DyJR on various mathematical benchmarks. *init* denotes the percentage of rollout samples retained per step during the initial 20 steps, while η represents the retention rate thereafter. The maximum age of the FIFO buffer is consistently set to 8 steps.

Model	AIME25	AMC23	Beyond AIME	BRUMO25	HMMT25	Minerva*	Avg
DyJR (<i>init</i> = 20%, η = 20%)	22.9	72.5	12.5	33.8	12.6	51.0	34.2
DyJR (<i>init</i> = 20%, η = 5%)	23.1	72.0	12.7	33.4	12.7	50.4	34.1
DyJR (<i>init</i> = 10%, η = 5%)	22.5	69.2	11.4	31.5	11.5	48.2	32.4
DyJR (<i>init</i> = 5%, η = 5%)	21.8	68.5	10.1	29.2	10.3	47.8	31.3

We evaluated whether maintaining a consistently large sample collection rate yields significant differences compared to our current strategy, with results presented in the Table 5. Our ablation study yields two critical observations regarding data utilization:

- Diminishing Returns of Late-Stage Data:** Maintaining a consistently high global sampling rate (0.2) implies no significant performance gain compared to our dynamic strategy. This suggests that as the model stabilizes in the mid-to-late stages, a minimal set of replay samples suffices to anchor the distribution, validating the memory efficiency of DyJR’s dynamic contraction.
- Criticality of Initial Data:** Conversely, reducing the sampling rate during the initial phase (*init*) results in a significant deterioration of performance.

Reevaluating Replay Value—Diversity Over Accuracy. These findings challenge the conventional understanding of Experience Replay. If the primary value of replayed data lay solely in its **correctness** (i.e., reinforcing accurate solutions to prevent forgetting), then late-stage trajectories—generated by a model with higher accuracy—should theoretically be more valuable than early-stage ones. However, our experiments reveal a paradox: **although the early-stage model exhibits lower accuracy, the data it generates is indispensable for final performance.** This contradiction strongly suggests that the

efficacy of DyJR stems not from merely cloning correct behaviors, but from preserving the **high entropy and reasoning diversity** inherent in early training. By leveraging these early, diverse trajectories as a distributional constraint via JS divergence, DyJR prevents the model from prematurely converging to a narrow solution path (mode collapse). Consequently, unlike static replay methods that simply mitigate forgetting, DyJR actively safeguards the model’s exploration capability, leading to substantial gains in Pass@1.